High-fidelity Computational Simulation to Refine Strategies for Lung-Protective Ventilation in Paediatric Acute Respiratory Distress Syndrome

Data Supplement

Sina Saffaran, MSc[1]; Anup Das, PhD[1]; Jonathan G. Hardman, PhD[2]; Nadir Yehya, MD[3]*; and Declan G. Bates, PhD[1]*

DETAILED METHODS

Patient Selection

Development cohort: Patients were selected from an ongoing (since 2011) observational prospective cohort [1] of intubated children meeting Berlin criteria for ARDS from the Children's Hospital of Philadelphia (CHOP). The study was reviewed by the CHOP Institutional Review Board, and requirement for informed consent was waived. As the cohort was initiated prior to publication of the PALICC definition of PARDS [2], we did not screen based on oxygenation index; however, all patients met PALICC criteria. Thirty subjects between 2.5 and 4 years of age ventilated via a 5.0 mm cuffed endotracheal tube during neuromuscular blockade were selected. We restricted the initial cohort to this age/size range to limit some of the variability during model development: e.g. we selected subjects with 5.0 mm internal diameter tracheal tubes, allowing consistency when calculating ventilatory resistance. Furthermore, this age range was close to the median age (4 years) of the overall cohort. Finally, we used paralyzed subjects to ensure reproducibility of the associations between ventilator changes and gas exchange, which would be confounded by spontaneous effort. Arterial blood gases (ABG) and ventilator changes during the first 72 hours of PARDS were recorded. The respiratory variables of peak inspiratory pressure (PIP), positive end-expiratory pressure (PEEP), and exhaled V_T were collected at the ventilator for patients with $V_T \geq 100$ mL using integrated software provided by the manufacturer (Dräger, Inc., Lübeck, Germany), and using a sensor proximate to the endotracheal tube for $V_T < 100$ mL. Ventilator management and use of ancillary therapies were not protocolized.

Test cohorts: To test the utility and generalisability of the model and associated ventilation strategies, we repeated the analyses in a separate cohort of children aged 1 to 2 years. This age group was selected because larger V_T are commonly used to overcome

perceived increases in dead space in younger lungs. Finally, we repeated analyses in a cohort of 19 children between 1 month and 18 years of age with V_T > 10 mL/kg, as we identified this as a subgroup in which lung-protective strategies may have the greatest impact.

Simulator Development

Analyses were carried out using a simulator that includes representations of multiple interacting organ systems, incorporates a high level of physiological detail, and has been extensively validated in several previous studies of adult ARDS [3-5]. The paediatric simulator was developed by performing a detailed revision of both the model structure and parameters in light of the key differences between paediatric and adult physiology. The core components of the computational simulator used in this study have been developed by our group over the past several years and have been validated on a number of previous studies of adult pathophysiology [6-8]. The model includes representations of multiple interacting organ systems and incorporates a high level of physiological detail (including multiple alveolar compartments, multi-compartmental gas-exchange, viscoelastic compliance behaviour, interdependent blood-gas solubility and haemoglobin behaviour and heterogeneous distributions of pulmonary ventilation and perfusion). Each model component is described as several mass conserving functions and solved as algebraic equations, obtained or approximated from the published literature, experimental data and clinical observations. These equations are solved in series in an iterative manner, so that solving one equation at current time instant determines the values of the independent variables in the next equation. At the end of the iteration, the results of the solution of the final equations determine the independent variables of the first equation for the next iteration.

The model simulates all relevant aspects of pulmonary dynamics and gas exchange, i.e. the transport of air from mouth to airway and alveoli, the gas exchange between alveoli

and their corresponding capillaries, and the gas exchange between blood and peripheral tissue. The model includes series dead space (i.e. conducting airways where there is no gas exchange) to represent the trachea, bronchi and the bronchioles. The lung model incorporates 100 independently configurable alveolar compartments, implemented in parallel. Multiple alveolar compartments allow the model to simulate alveolar shunt and alveolar dead space in detail. Figure S1 shows a simplified, diagrammatic representation of the model components and their interactions.

There are a number of important differences between adult and paediatric pulmonary physiology. Some physiological features such as lung volume, cardiac output, oxygen consumption, airway resistance and pulmonary vascular resistance are highly variable in children depending on their age and weight. Thus, cardiac output and the volume of functional residual capacity are estimated in the model using the following equations:

$$CO = 933 \times weight_{(kg)}^{0.38} \qquad (ml.min^{-1}) \tag{1}$$

$$V_{frc} = 9.51 \times weight_{(kg)}^{1.31} \qquad (ml) \tag{2}$$

The total airway resistance and pulmonary vascular resistance are greater in children than in adults, decreasing as they grow older. The specific airway resistance can be estimated by:

$$sR_{tot} = 1.3083378 - 0.00016486 * age^3 - 0.03670306 * sex \qquad (kPa.s) \tag{3}$$

where sex is set to 1 for males and 0 for females. The total resistance is calculated as:

$$R_{tot} = \frac{sR_{tot}}{V_{frc}} \qquad (kPa.s.l^{-1}) \tag{4}$$

and is distributed between the main airway and 100 parallel alveolar compartments in the model. Every alveolar compartment also has two resistances placed in series, namely the alveolar inlet resistance and the upper bronchial resistance. The pulmonary vascular resistance (PVR) is calculated by means of the following equation:

$$PVR = \frac{80(MPAP - MPCWP)}{CO} \qquad (\frac{dyn.s}{cm^5}) \tag{5}$$

Note that the difference in values for mean pulmonary arterial pressure (MPAP) and mean pulmonary capillary wedge pressure (MPCWP) is virtually identical in children and adults. Hence, lower cardiac output plays the main role in generating higher PVR values for paediatric subjects. In the model, each single alveolar compartment is characterized by four individually configurable parameters. These four parameters represent the alveolar compartment inlet resistance, the extrinsic pressure acting on the compartment, the stiffness of the compartment and the threshold opening pressure of the compartment, which are annotated as R_{comp}, P_{ext}, k_{stiff} *and TOP* respectively. Selection of varying values for each of these four parameters across the 100 alveolar compartments in the model allows the accurate representation of the heterogeneous nature of diseased lungs.

Simulator Calibration to Patient Data

The model was calibrated against the individual patient data on arterial blood gas contents, airway pressures and ventilator settings for each patient in the PARDS dataset using an optimization approach. The model parameters (x) that were used in the optimization include the four key alveolar features mentioned previously (R_{comp}, P_{ext}, k_{stiff} *and TOP*) for all 100 alveolar compartments, as well as values for the inspiratory duty cycle (DC), respiratory quotient (RQ), total oxygen consumption (VO2), respiratory rate (RR, when not available), haemoglobin (Hb), volume of anatomical dead space (V_D) and anatomical shunt ($Shunt_{anat}$). The optimization problem is formulated to find the configuration of model parameters (x) that minimize the difference between the model outputs (for a given set of ventilator settings) and the patient data. This error is captured by a cost function J given below:

$$\min_x J = \sqrt{\sum_{i=1}^{7} \frac{\hat{Y}_i - Y_i}{Y_i}} \quad (6)$$

where

$$Y = [PaO_2, PaCO_2, P_E{}'CO_2, PIP, mPaw, TOP_{mean}, V_{frc}] \quad (7)$$

Y is a vector of data values and $\hat{Y}$ is the model estimated values. The average threshold opening pressure of all the compartments (TOP_{mean}) is optimized to be 20 cmH_2O. Table S1 presents a summary of the parameters included in (x), with their dimensions and allowable range of variation. The values of the model parameters (x) that produced the closest match to the patient data were found by using a Genetic Algorithm (GA), a global optimization method.

Strategies for Achieving Lung-Protective Ventilation

After matching the model to each individual patient, the potential for achieving lung-protective ventilation in these patients was investigated by evaluating four different strategies on each of the virtual patients. The primary objective was to progressively lower the risk of VILI without violating the following safety constraints:

$P_aO_2 \geq 8$ (60)	kPa (mmHg)
$P_aCO_2 \leq 8$ (60)	kPa (mmHg)
PIP ≤ 35	cmH_2O
RR ≤ 40	bpm

P_aO_2, P_aCO_2 and RR are partial pressure of oxygen in arterial blood, partial pressure of carbon dioxide in arterial blood and respiratory rate, respectively. These constraints are based on those used in clinical trials in adult ARDS, adapted to match the requirements of paediatrics [9, 10]. In cases where the data indicated that a patient's initial settings did not comply with one or more of the aforementioned safety criteria, an attempt to reduce VILI was

only made if it led to an improvement in the patient's safety parameters (e.g. reducing P_aCO_2 or PIP). The four strategies were designed using volume control mode (VC-CMV) and based on physiological equations that are widely used in clinical practice, as follows:

Strategy 1: V_T was reduced in steps of 0.5 mL/kg with each step lasting for 30 minutes. ABG and PIP were checked at the end of each phase until any further reduction violated one of the above constraints. RR was simultaneously adjusted at each step to maintain a constant minute ventilation (MinV) using:

$$MinV = V_T \times RR \tag{1}$$

Strategy 2: Alveolar minute ventilation ($MinV_{alv}$) was kept constant instead of the general MinV. To do this, the amount of anatomical dead space (V_D) must be taken into account, and thus $MinV_{alv}$ was calculated from the equation [11-13]:

$$MinV_{alv} = (V_T - V_D) \times RR \tag{2}$$

Strategy 3: Here, a strategy previously employed in [14, 15] was implemented in the simulator. In this approach, the $MinV_{alv}$ was kept constant using Eq.2, and the inspiratory flow kept constant using the equation:

$$F_{insp} = \frac{V_T \times RR}{60 \times DC} \tag{3}$$

where F_{insp} is the square inspiratory flow into the lung from the ventilator (no pause time used), and DC is duty cycle. As V_T and RR had already been determined (same as strategy 2), F_{insp} could only be manipulated by varying DC in Eq.3. Thus, the difference between strategies 2 and 3 is that DC is set as constant for the former, while DC is adjusted to maintain a constant F_{insp} in the latter.

Strategy 4: A recent study of adult ARDS [16] suggested that reductions in V_T are most advantageous when accompanied by a corresponding decrease in ΔP, defined as the difference between plateau pressure (P_{plat}) and PEEP. P_{plat} is calculated directly from the simulator and represents the end inspiratory lung pressure. The strategy for decreasing ΔP works by increasing PEEP and adjusting V_T to keep the plateau pressure constant. For this purpose, PEEP was increased by 1 cmH_2O (causing a rise in P_{plat}) and then V_T was reduced in steps of 0.5 mL/kg until P_{plat} returned to its initial value. The procedure was then repeated until one of the safety constraints was violated.

Additional Variables Collected

We also recorded strain, strain rate, and mechanical power. Dynamic and static strain are markers of mechanical load during ventilation and assist with understanding how the whole lung is affected by ventilation [17-19]. Although it is not possible to measure exact values of strain in clinical practice, in the simulator they can be estimated as $V_T/V_{frc(ZEEP)}$ for dynamic strain and $V_{PEEP}/V_{frc(ZEEP)}$ for static strain, where V_{PEEP} is the volume of gas in the lung due to PEEP and $V_{frc(ZEEP)}$ is the volume of functional residual capacity when PEEP is zero [17]. Mechanical power was calculated using the equation [20]:

$$Power_{rs} = 0.098 \times RR \times \left\{ {V_T}^2 \times \left[0.5 \times EL_{rs} + RR \times \frac{(1 + I{:}E)}{60 \times I{:}E} \times R_{aw} \right] + V_T \times PEEP \right\} \quad (4)$$

Where EL_{rs} is the elastance of the respiratory system, I:E is the inspiratory-to-expiratory time ratio, and R_{aw} is the airway resistance.

Statistical Analysis

Data are presented as mean ± SD, or graphed using median, interquartile and total ranges. Data for all subjects, even those in whom VILI reductions could not be performed without violating safety constraints, was presented. To avoid violation of underlying

distribution assumptions, variables were compared using nonparametric statistics when, including Spearman's rho, signed-rank test, rank-sum test, and Kruskal–Wallis. Two-sided $p < 0.05$ was considered significant.

COMPLETE RESULTS

The Simulator Accurately Represents Patient Data

The ability of the simulator to accurately reproduce patient data was verified by comparing its responses against data on the responses (P_aO_2 and $P_aCO_2$values) of 30 patients in the development cohort to mechanical ventilation. No strong correlation was observed between the reported values of V_T (Kruskal-Wallis $p = 0.7$), PEEP ($p = 0.4$) and RR ($p = 0.3$) and PARDS severity category. Individual and average data across the cohort are shown in Table S2. At baseline, 2 patients had $V_T > 10$ mL/kg, 10 patients had V_T 8–10 mL/kg, 16 had V_T 6–8 mL/kg, and 2 had $V_T < 6$ mL/kg.

After model calibration, each individual patient was simulated for 30 minutes (or until reaching steady-state) under ventilation with constant flow in the supine position. Figure 1-(a) and 1-(b) compares the outputs of the simulator with the original data, expressed as median, interquartile range and actual range for the entire cohort (see also Figure S2). Figure 1-(c) to 1-(f) plot the data points versus simulator output values. These results confirm the capability of the simulator to accurately replicate multiple output values of the patients included in the cohort dataset across a range of different ventilator settings.

Evaluating Strategies for Implementing Protective Ventilation

Figure S3 shows the effect of each strategy for implementing protective ventilation, in terms of its effect on V_T, alveolar dynamic strain, mechanical power and ΔP. Similar reductions in average V_T across were achieved using strategies 1 to 3 (15% (1.3 mL/kg), 12%

(1 mL/kg) and 14% (1.2 mL/kg), respectively). RR needed to be increased by a smaller amount (15%) for strategy 1, (versus 33% and 37% on average for strategies 2 and 3, respectively). After implementing any of these three strategies, the number of patients being ventilated using V_T > 10 mL/kg fell to zero. There were also reductions in the number of patients receiving V_T in the ranges of 8–10 mL/kg (-30 % for all strategies) and 6–8 mL/kg (-18.8% for strategies 1 and 3, -12.5% for strategy 2). Correspondingly, the number of patients receiving V_T in the range 4–6 mL/kg rose from 6.7% to 33.3% in strategy 1 and to 30% in strategies 2 and 3, respectively. These average reductions were achieved despite the fact that there were 8 patients (4 severe PARDS, 4 moderate PARDS) whose baseline values of P_aCO_2 and PIP did not allow any of the strategies to be implemented without violating constraints.

Figure S3 shows significant reductions in dynamic strain for strategies 1 to 3 (-20%, -19% and -19%, respectively) with corresponding increases in static strain (+9%, +17% and +35%, respectively; Figure S4). The rise in static strain indicates larger lung volumes at end-expiration. In strategy 3, the change in DC (shorter exhalation time) explains the higher static strain compared to strategies 1 and 2. To rule out the possibility that higher static strains are due to breath-stacking, the difference between the inhaled V_T (V_{T_i}) and exhaled V_T (V_{T_e}) were examined in all strategies to detect possible incomplete exhalation. The change in end-expiratory lung volume was also monitored over a 3-hour time period. Both investigations confirm that the higher static strains are not a result of breath-stacking (Figure S5).

Differences emerged when considering the effect of each strategy on mechanical power. Strategy 1 produced no significant change (+1%; $p = 0.2$, signed-rank test) but both strategies 2 and 3 resulted in large increases (+22% and +19%, respectively; both $p < 0.05$). Amongst the four safety constraints, limits on P_aCO_2 and RR played the main role in restricting further reduction of V_T. Limits on P_aO_2 were never reached.

When strategy 4 (adjusting PEEP and V_T to reduce ΔP) was applied, the P_aCO_2 limit was the only constraint precluding further reductions due to the strategy not compensating for MinV. Maintaining MinV is not possible using this strategy, as it requires increasing RR, leading to a rise in P_{plat} which in turn impedes reduction of ΔP. Consequently, this approach was only able to reduce ΔP in the 13 patients with the lowest initial P_aCO_2 levels. The average reduction in ΔP was -6% for all 30 patients in the cohort and -17% for the 13 patients on which this strategy could be applied. The corresponding changes in V_T and PEEP were -7% and +10% respectively. This compares with changes in ΔP of -4%, +1% and +8% for strategies 1-3, respectively. Strategy 4 was the only approach that produced a significant reduction in mechanical power (-8%, versus +1%, +22% and +19% for strategies 1-3).

Additional Test Cohorts

To test the utility and generalisability of our results, we applied the same 4 strategies to two separate test cohorts of PARDS patients from the CHOP dataset. For both test cohorts, the same fidelity in matching simulated outputs to patient data was observed as with the initial development cohort. Two patients in Test Cohort 1 and three patients in Test Cohort 2 had baseline values of P_aCO_2 and PIP that would not allow any of the proposed strategies to be implemented.

Similar trends emerged in terms of achieving more protective ventilation for all 4 strategies (Figures S6-7). Strategy 1 produced the largest reductions in V_T (-22% in Test Cohort 1, -28% in Test Cohort 2) and dynamic strain (-20% in Test Cohort 1, -27% in Test Cohort 2), with the lowest corresponding increase in static strain (+1% in Test Cohort 1, +3% in Test Cohort 2). Strategy 1 produced a small reduction in mechanical power (-4% in both cohorts) and significant reductions in ΔP (-13% and -16%). While strategies 2 and 3 achieved reductions in V_T, ΔP, and dynamic strain, this came at the cost of higher increases in static

strain than required by strategy 1. Both strategies 2 and 3 also produced large increases in power. Finally, strategy 4 produced significant decreases in V_T, dynamic strain and ΔP in both test cohorts, and the largest decreases in power (-10% in Test Cohort 1, -23% in Test Cohort 2). Over the three cohorts analysed, Test Cohort 2 (initial $V_T > 10$ mL/kg) showed the greatest potential for improvements in terms of achieving more protective ventilation.

ADDITIONAL DISCUSSION

We have developed and tested four separate strategies for achieving lung protective ventilation in PARDS. A strategy of maintaining MinV allowed for greatest reduction in V_T with small decreases in mechanical power. A strategy of minimizing ΔP resulted in larger reductions in mechanical power, with smaller reductions in V_T. Conversely, strategies aimed at maintaining constant alveolar ventilation, either by manipulating DC or inspiratory flow, are capable of reducing V_T and ΔP, they come at the expense of increasing power. Although previous studies utilising a uniform low V_T showed deleterious effects [21], here V_T was progressively reduced in patients only as long as it did not violate safety constraints on gas exchange.

In 2015, PALICC released the first recommendations specifically for PARDS [2], and addressed several issues in patient treatment. Strategies limiting V_T and plateau pressure achieved "weak agreement." In addition, a survey on practice patterns found that although paediatricians theoretically concurred with adult guidelines to use lower V_T and pressures, in actual practice, over 25% of PARDS patients are ventilated with $V_T > 10$ mL/kg [22], and likely higher in obese children when adjusting for ideal body weight [23]. Despite this, mortality rates in PARDS have improved over the last two decades, part of which may be related to adoption of lung-protective ventilation strategies. Continued resistance to lung-protective ventilation, particularly use of $V_T > 10$ mL/kg, may reflect concerns regarding

whether V_T and ventilator pressures can be safely reduced in this population. We have demonstrated here the feasibility of adjusting ventilator settings to mitigate VILI within reasonable safety parameters for gas exchange and RR. The reductions achieved are most pronounced in subjects with V_T > 10 mL/kg, and appear to be generalizable throughout the entire age range and severity encountered in PARDS. While studies of ΔP and mechanical power limits are in their infancy, preliminary data suggest "thresholds" above which these values are associated with worse outcomes [24, 25]. Analysis of our dataset shows that these thresholds are currently being exceeded in many subjects, particularly in children with V_T > 10 mL/kg.

Static strain represents the initial displacement of the lungs from their original position due to PEEP at the start of ventilation and subsequently stays constant during ventilation unless PEEP is changed. It has been shown that the lung can tolerate increased static strain, provided that the total lung capacity is not exceeded, and that dynamic strain is likely to be more injurious [17, 19]. The change in lung strain is also correlated with the recruited volume of the lung. A recent study showed that lung recruitment causes reduction in dynamic strain while increasing static strain [19]. Hence, both the changes in static and dynamic strain observed in our results suggest general improvement in lung recruitment as a result of the changes to ventilator settings.

Strategy 4 resulted in reduced mechanical power. The original power equation (Eq. 4) by Gattinoni et al. [20] can be simplified and re-written as the equation below (Section S8 in the Supplemental File):

$$Power_{rs} = RR \times V_T \times \left(P_{peak} - 0.5P_{plat} + 0.5PEEP\right) = RR \times V_T \times (P_{peak} - 0.5\Delta P) \qquad (5)$$

Considering the above equation, it can be expected that an increment in inspiratory flow (Eq. 3) leads to an increase in power as long as the cause of the change in flow is MinV (i.e. $RR \times V_T$). However, when MinV was kept constant and a smaller DC raised the flow, the resultant

change in power depends on how P_{peak} and P_{plat} respond to the adjustment – i.e. specifically the change of $P_{peak} - 0.5\Delta P$. As a result, it cannot be concluded that a greater flow would always lead to a rise in the power. Moreover, it should be noted that MinV directly impacts the power, not the flow itself. For instance, patients were ventilated with the same flow in strategy 1 and strategy 3, while the latter has a larger MinV, thus higher power.

The study has a number of limitations. Data were derived from a single institution, and while severity of PARDS and outcomes were similar to other cohorts, generalizability remains to be demonstrated. To minimise possible confounding factors, the model was configured to represent patients that are fully sedated under mechanical ventilation; therefore autonomic reflex modules in the model were not utilised. The model also does not include the effect of inflammatory mediators commonly found in PARDS, which are difficult to quantify and isolate in clinical settings. As the model is computational in nature, it does not provide any direct histological or biological evidence of the effects of the proposed ventilation strategies on VILI markers, and therefore further animal and/or human studies should be performed to provide conclusive evidence of their relative effectiveness in achieving more protective ventilation. As adolescents may be diagnosed with either Berlin or PALICC criteria [26], it is unclear whether they would be more appropriately managed with our protocol, or an adult version. The model was developed to focus on ventilator settings affecting VILI, and thus we chose to set constraints on PaCO2, rather than pH, which is often modified by entire non-ventilator interventions, such as volume resuscitation or exogenous bicarbonate.

REFERENCES

1. Yehya N, Servaes S, Thomas NJ, (2015) Characterizing degree of lung injury in pediatric acute respiratory distress syndrome. Crit Care Med 43: 937-946
2. Khemani RG, Smith LS, Zimmerman JJ, Erickson S, Pediatric Acute Lung Injury Consensus Conference G, (2015) Pediatric acute respiratory distress syndrome: definition, incidence, and epidemiology: proceedings from the Pediatric Acute Lung Injury Consensus Conference. Pediatr Crit Care Med 16: S23-40
3. Das A, Menon PP, Hardman JG, Bates DG, (2013) Optimization of mechanical ventilator settings for pulmonary disease states. IEEE transactions on bio-medical engineering 60: 1599-1607
4. Das A, Cole O, Chikhani M, Wang W, Ali T, Haque M, Bates DG, Hardman JG, (2015) Evaluation of lung recruitment maneuvers in acute respiratory distress syndrome using computer simulation. Crit Care 19: 8
5. Chikhani M, Das A, Haque M, Wang W, Bates DG, Hardman JG, (2016) High PEEP in acute respiratory distress syndrome: quantitative evaluation between improved arterial oxygenation and decreased oxygen delivery. British journal of anaesthesia 117: 650-658
6. Hardman JG, Bedforth NM, Ahmed AB, Mahajan RP, Aitkenhead AR, (1998) A physiology simulator: validation of its respiratory components and its ability to predict the patient's response to changes in mechanical ventilation. British journal of anaesthesia 81: 327-332
7. Bedforth NM, Hardman JG, (1999) Predicting patients' responses to changes in mechanical ventilation: a comparison between physicians and a physiological simulator. Intensive Care Med 25: 839-842
8. Das A, Gao Z, Menon PP, Hardman JG, Bates DG, (2011) A systems engineering approach to validation of a pulmonary physiology simulator for clinical applications. J R Soc Interface 8: 44-55
9. Acute Respiratory Distress Syndrome N, Brower RG, Matthay MA, Morris A, Schoenfeld D, Thompson BT, Wheeler A, (2000) Ventilation with lower tidal volumes as compared with traditional tidal volumes for acute lung injury and the acute respiratory distress syndrome. N Engl J Med 342: 1301-1308
10. Brower RG, Lanken PN, MacIntyre N, Matthay MA, Morris A, Ancukiewicz M, Schoenfeld D, Thompson BT, National Heart L, Blood Institute ACTN, (2004) Higher versus lower positive end-expiratory pressures in patients with the acute respiratory distress syndrome. N Engl J Med 351: 327-336
11. Nuckton TJ, Alonso JA, Kallet RH, Daniel BM, Pittet JF, Eisner MD, Matthay MA, (2002) Pulmonary dead-space fraction as a risk factor for death in the acute respiratory distress syndrome. N Engl J Med 346: 1281-1286
12. Beitler JR, Thompson BT, Matthay MA, Talmor D, Liu KD, Zhuo H, Hayden D, Spragg RG, Malhotra A, (2015) Estimating dead-space fraction for secondary analyses of acute respiratory distress syndrome clinical trials. Crit Care Med 43: 1026-1035
13. Yehya N, Bhalla AK, Thomas NJ, Khemani RG, (2016) Alveolar Dead Space Fraction Discriminates Mortality in Pediatric Acute Respiratory Distress Syndrome. Pediatr Crit Care Med 17: 101-109
14. Wang W, Das A, Cole O, Chikhani M, Hardman JG, Bates DG, (2015) Computational simulation indicates that moderately high-frequency ventilation can allow safe reduction of tidal volumes and airway pressures in ARDS patients. Intensive Care Med Exp 3: 33

15. Cordioli RL, Park M, Costa EL, Gomes S, Brochard L, Amato MB, Azevedo LC, (2014) Moderately high frequency ventilation with a conventional ventilator allows reduction of tidal volume without increasing mean airway pressure. Intensive Care Med Exp 2: 13
16. Amato MB, Meade MO, Slutsky AS, Brochard L, Costa EL, Schoenfeld DA, Stewart TE, Briel M, Talmor D, Mercat A, Richard JC, Carvalho CR, Brower RG, (2015) Driving pressure and survival in the acute respiratory distress syndrome. N Engl J Med 372: 747-755
17. Protti A, Votta E, Gattinoni L, (2014) Which is the most important strain in the pathogenesis of ventilator-induced lung injury: dynamic or static? Curr Opin Crit Care 20: 33-38
18. Protti A, Maraffi T, Milesi M, Votta E, Santini A, Pugni P, Andreis DT, Nicosia F, Zannin E, Gatti S, Vaira V, Ferrero S, Gattinoni L, (2016) Role of Strain Rate in the Pathogenesis of Ventilator-Induced Lung Edema. Crit Care Med 44: e838-845
19. Garcia-Prieto E, Lopez-Aguilar J, Parra-Ruiz D, Amado-Rodriguez L, Lopez-Alonso I, Blazquez-Prieto J, Blanch L, Albaiceta GM, (2016) Impact of Recruitment on Static and Dynamic Lung Strain in Acute Respiratory Distress Syndrome. Anesthesiology 124: 443-452
20. Gattinoni L, Tonetti T, Cressoni M, Cadringher P, Herrmann P, Moerer O, Protti A, Gotti M, Chiurazzi C, Carlesso E, Chiumello D, Quintel M, (2016) Ventilator-related causes of lung injury: the mechanical power. Intensive Care Med 42: 1567-1575
21. Eichacker PQ, Gerstenberger EP, Banks SM, Cui X, Natanson C, (2002) Meta-analysis of acute lung injury and acute respiratory distress syndrome trials testing low tidal volumes. Am J Respir Crit Care Med 166: 1510-1514
22. Santschi M, Randolph AG, Rimensberger PC, Jouvet P, Pediatric Acute Lung Injury Mechanical Ventilation I, Pediatric Acute Lung I, Sepsis Investigators N, European Society of P, Neonatal Intensive C, (2013) Mechanical ventilation strategies in children with acute lung injury: a survey on stated practice pattern*. Pediatr Crit Care Med 14: e332-337
23. Ward SL, Quinn CM, Valentine SL, Sapru A, Curley MA, Willson DF, Liu KD, Matthay MA, Flori HR, (2016) Poor Adherence to Lung-Protective Mechanical Ventilation in Pediatric Acute Respiratory Distress Syndrome. Pediatr Crit Care Med 17: 917-923
24. Serpa Neto A, Deliberato RO, Johnson AEW, Bos LD, Amorim P, Pereira SM, Cazati DC, Cordioli RL, Correa TD, Pollard TJ, Schettino GPP, Timenetsky KT, Celi LA, Pelosi P, Gama de Abreu M, Schultz MJ, Investigators PN, (2018) Mechanical power of ventilation is associated with mortality in critically ill patients: an analysis of patients in two observational cohorts. Intensive Care Med 44: 1914-1922
25. Laffey JG, Bellani G, Pham T, Fan E, Madotto F, Bajwa EK, Brochard L, Clarkson K, Esteban A, Gattinoni L, van Haren F, Heunks LM, Kurahashi K, Laake JH, Larsson A, McAuley DF, McNamee L, Nin N, Qiu H, Ranieri M, Rubenfeld GD, Thompson BT, Wrigge H, Slutsky AS, Pesenti A, Investigators LS, the ETG, (2016) Potentially modifiable factors contributing to outcome from acute respiratory distress syndrome: the LUNG SAFE study. Intensive Care Med 42: 1865-1876
26. De Luca D, (2018) Personalising care of acute respiratory distress syndrome according to patients' age. The Lancet Respiratory medicine

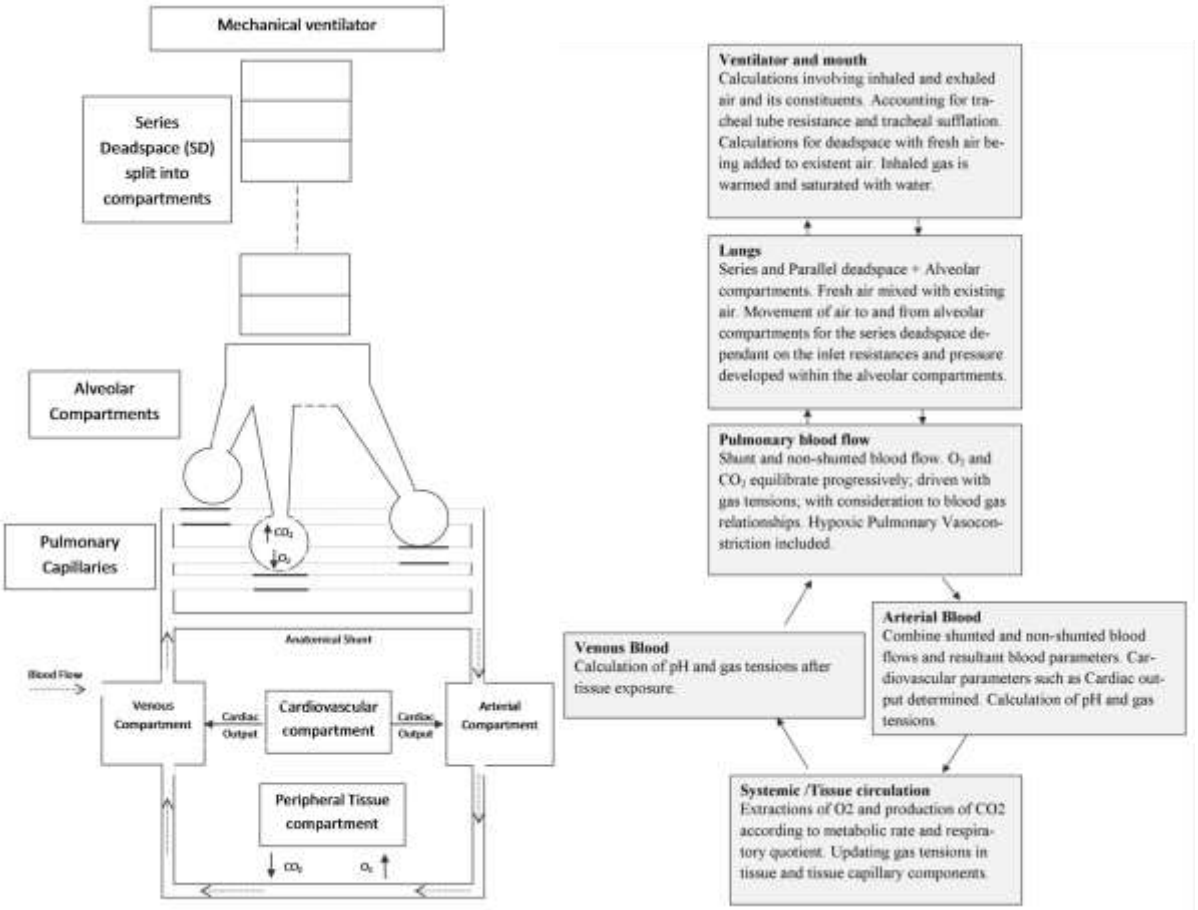

Figure S1: A simplified, diagrammatic representation of the model. The model includes representations of multiple interacting organ systems and incorporates an unprecedented level of physiological detail; including multiple alveolar compartments, multi-compartmental gas-exchange, viscoelastic compliance behaviour, interdependent blood-gas solubility and haemoglobin behaviour and heterogeneous distributions of pulmonary ventilation and perfusion.

Table S1: List of the parameters varied by the optimization algorithm in order to calibrate the model to patient data, with their dimensions and allowable range of variation.

Parameter (x)	size	ranges
P_{ext}	100	[-50,20]
k_{stiff}	100	[-1,2]
TOP (cmH_2O)	100	[0,100]
RQ	1	[0.7,0.9]
Duty Cycle	1	[0.3 0.4]
VO_2 ($mL.min^{-1}$)	1	[40,200]
RR^* ($b.min^{-1}$)	1	[20,40]
Hb ($g.l^{-1}$)	1	[90,160]
$Shunt_{anat}$ (%)	1	[1,2]
VD_{anat} (mL)	1	[20,200]

P_{ext}: the extrinsic pressure acting on compartments; k_{stiff}: the stiffness of the compartments; TOP: threshold opening pressure of the compartments; RQ: respiratory quotient; VO_2: total oxygen consumption; RR: respiratory rate; Hb: hemoglobin; V_D: volume of anatomical dead space; $Shunt_{anat}$: anatomical shunt.

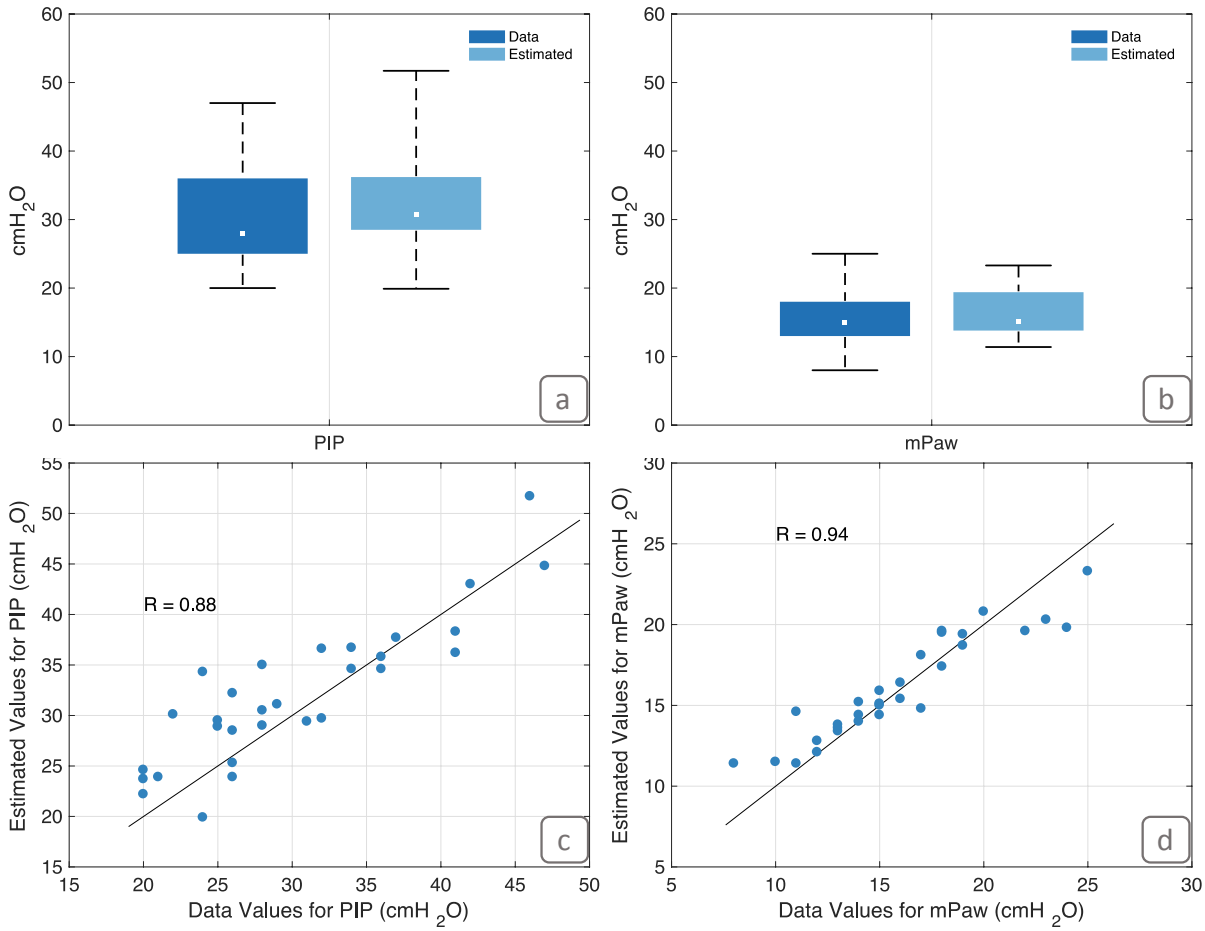

Figure S2: Results of the extended model validation on the development cohort by comparing the patient data against simulator predicted values expressed as median, interquartile range and actual range: Panel (a) shows the result for leaving PIP out of the model matching and subsequently predicting its value; Panel (b) shows the result for leaving mPaw out of the model matching and subsequently predicting its value. In (c) and (d) data points are plotted versus predicted values, and R is the Spearman's rank correlation coefficient. PIP: peak inspiratory pressure; mPaw: mean airway pressure.

Table S2: Patient characteristics and mechanical ventilator settings for each individual patient in the development cohort, and as mean and standard deviations (SD) across the cohort.

ID	Age	Wgt	PRISM	Die	FiO_2	RR	V_T	PEEP	PF	OI	PaO_2	$P_E'CO_2$	$PaCO_2$	PIP	mPa
	y	kg				bpm	mL/kg	cmH_2O				mmHg		cmH_2O	
# 1	2.8	15	8	N	0.45	28	6.7	6	137	8	62	39	46	20	11
# 2	2.8	14	4	N	0.5	20	6.3	14	152	14.5	76	54	72	34	22
# 3	2.8	14.5	17	N	0.6	25	6.8	10	97	15.5	58	42	60	25	15
# 4	2.8	17	18	N	0.5	20	4.5	10	236	5.9	118	37	53	26	14
# 5	2.8	20	4	N	0.21	26	7	10	295	5.1	62	32	32	26	15
# 6	3	9.5	20	N	1	40	8.9	8	78	16.7	78	62	65	22	13
# 7	3	15	18	N	0.5	30	8.7	5	118	6.8	59	37	40	20	8
# 8	3	13.6	0	N	0.5	16	7.4	10	178	7.3	89	43	59	21	13
# 9	3	15	24	N	0.3	24	5.3	10	266	6.4	80	50	56	28	17
# 10	3	13	6	N	0.4	28	7.8	12	230	7	92	59	60	25	16
# 11	3.3	15	16	Y	0.5	25	7.5	8	178	7.3	89	43	46	26	13
# 12	3.5	14	14	N	0.35	34	10.3	8	274	5.1	96	54	56	28	14
# 13	4	17.5	0	N	0.55	20	6.9	10	149	10.1	82	43	72	29	15
# 14	4.3	19	12	N	0.6	24	7.2	14	111	18	67	41	56	41	20
# 15	2.5	12.2	1	N	0.3	26	8.9	12	343	5.2	103	60	63	32	18
# 16	3.7	15	13	N	0.4	22	6.7	6	170	5.9	68	48	51	24	10
# 17	3.3	14	5	Y	0.55	35	6.5	15	118	21.2	65	55	74	47	25
# 18	2.8	27	18	N	0.8	24	6.7	12	73	24.7	59	33	42	32	18
# 19	2.9	12	15	N	1	32	7.5	10	72	23.6	72	42	48	34	17
# 20	3	9.5	20	N	1	37	8.9	12	78	29.5	78	50	79	42	23
# 21	3	15	18	N	0.8	21	8.7	8	79	17.7	63.2	39	45	31	14
# 22	3	13.6	0	N	1	20	9.6	8	57	26.3	57	30	39	24	15
# 23	3	15	24	N	0.7	30	8	12	130	18.5	91	30	33	46	24
# 24	3	13	9	N	0.4	27	7.5	12	150	12.7	60	72	75	41	19
# 25	3.1	13	6	N	0.55	27	8.1	12	129	14.0	70.95	59	65	36	18
# 26	3.1	13	9	N	0.75	21	8.8	8	112	10.7	84	62	64	20	12
# 27	3.2	13	27	Y	1	23	7.7	7	59	18.6	59	20	34	28	11
# 28	3.3	15.5	7	N	0.35	23	8.4	8	237	6.8	82.95	47	59	36	16
# 29	3.3	15	7	N	0.6	24	7.5	6	108	11.1	64.8	26	38	26	12
# 30	3.5	14	5	Y	0.35	20	13.6	12	226	8.4	79.1	35	36	37	19
Mea	3.1	14.7	11.5	-	0.6	25.9	7.8	9.8	154.7	13.0	75.5	44.8	53.9	30.	15.9
SD	0.4	3.2	7.8	-	0.2	6.0	1.6	2.6	76.7	7.1	15.2	12.2	13.6	7.7	4.2

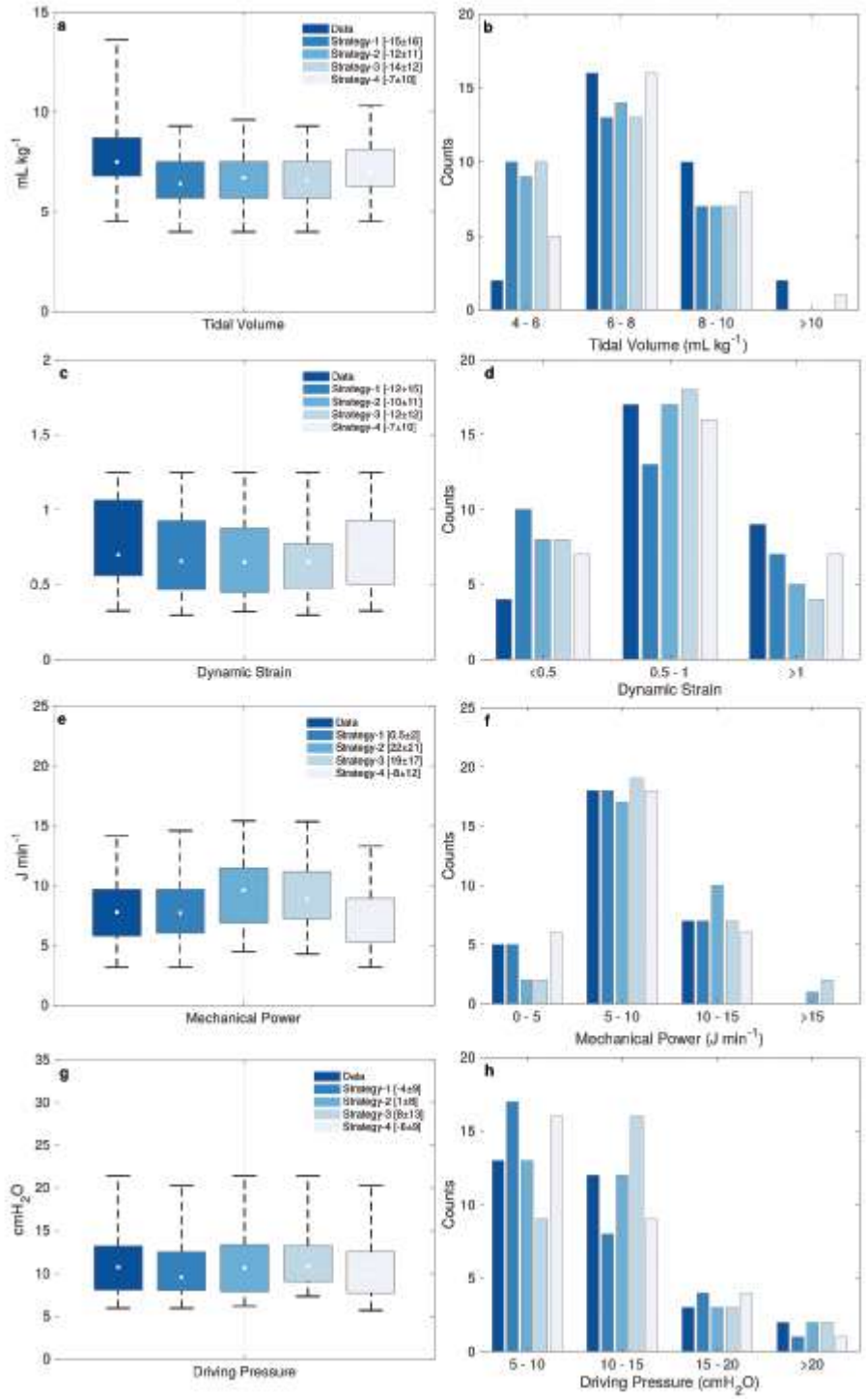

Figure S3: Development Cohort, box plots on the left show data as median, interquartile range and actual range while histograms on the right demonstrate the distribution of all patients' data before and after implementing different strategies. Numbers in the brackets are the average percentage change across the cohort [mean±SD]. Panels illustrate the amount of

tidal volume reduction (a)-(b), comparison of the alveolar dynamic strain (c)-(d), change in mechanical power (e)-(f) and driving pressure (g)-(h). Strategy-1: Reducing V_T whilst maintaining the initial minute ventilation; Strategy-2: Reducing V_T whilst maintaining the initial alveolar minute ventilation; Strategy-3: Reducing V_T whilst maintaining both the initial alveolar minute ventilation and inspiratory flow; Strategy-4: Reducing ΔP by increasing PEEP and decreasing V_T.

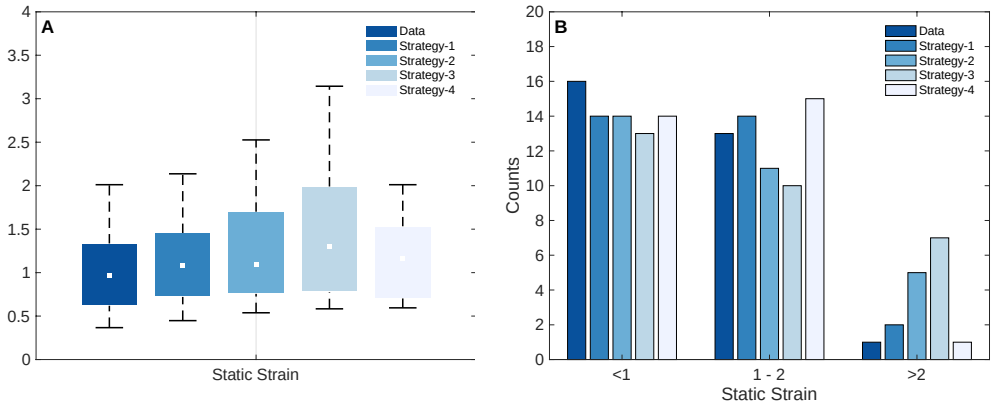

Figure S4: Comparison of the alveolar static strain before and after implementing the four strategies; expressed as median, interquartile range and actual range, (a). The distributions of patients' static and dynamic strains before after applying all the strategies are shown in (b).

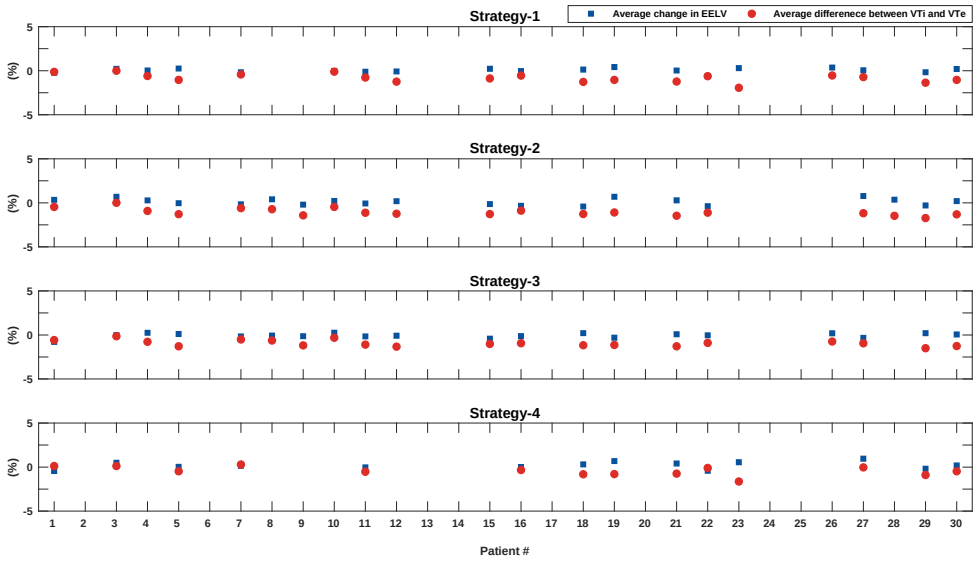

Figure S5: Figure shows the difference between the average inhaled tidal volumes (V_{T_i}) exhaled tidal volumes (V_{T_e}) (red circles) as well as the change in end-expiratory lung volume (EELV) over a 3h time period (blue squares).

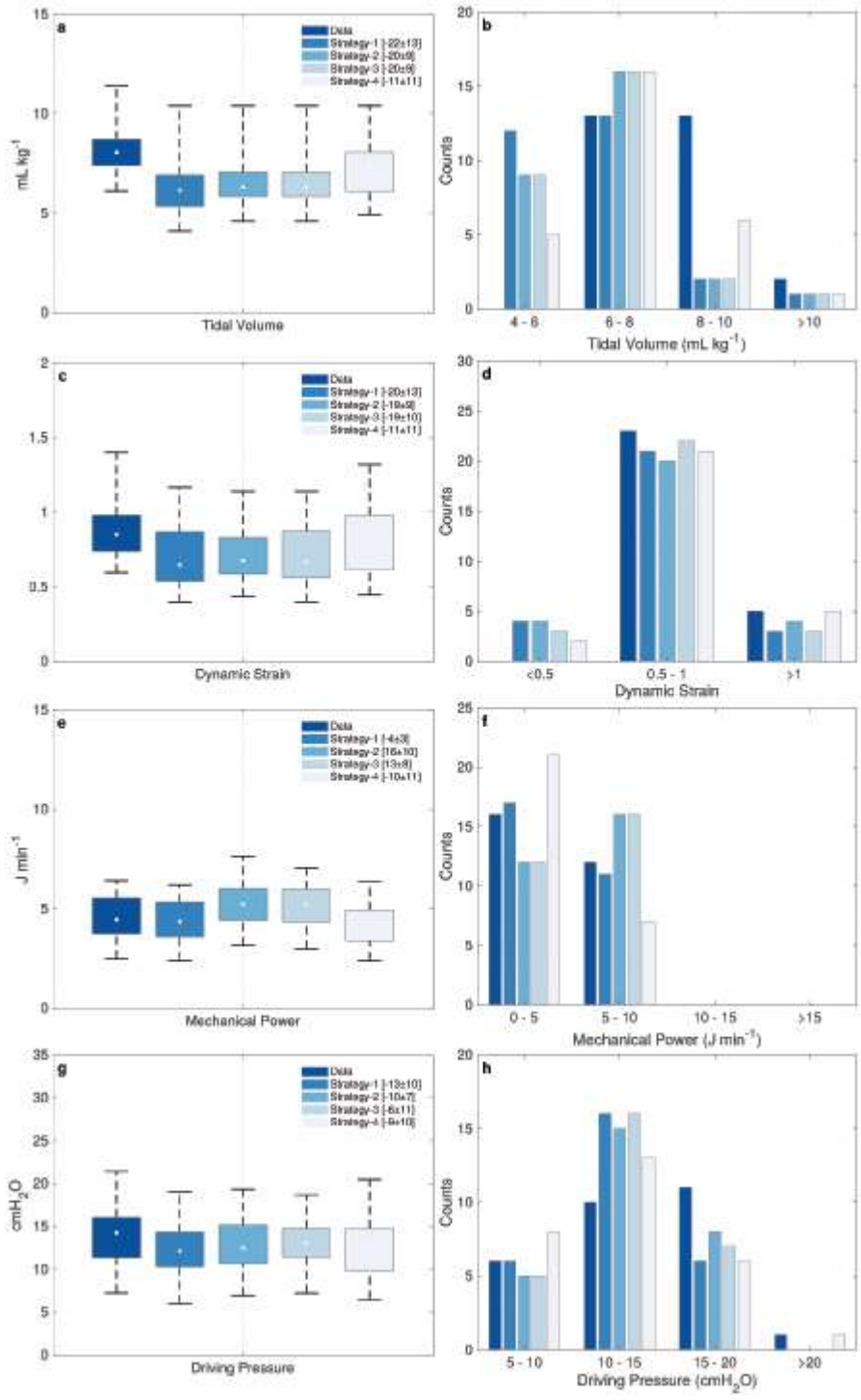

Figure S6: Test Cohort 1, box plots on the left show data as median, interquartile range and actual range while histograms on the right demonstrate the distribution of all patients' data before and after implementing different strategies. Numbers in the brackets are the percentage of average change across the cohort [mean±SD]. Panels illustrate the amount of tidal volume reduction (a)-(b), comparison of the alveolar dynamic strain (c)-(d), change in

mechanical power (e)-(f) and driving pressure (g)-(h). Strategy-1: Reducing V_T whilst maintaining the initial minute ventilation; Strategy-2: Reducing V_T whilst maintaining the initial alveolar minute ventilation; Strategy-3: Reducing V_T whilst maintaining both the initial alveolar minute ventilation and inspiratory flow; Strategy-4: Reducing ΔP by increasing PEEP and decreasing V_T.

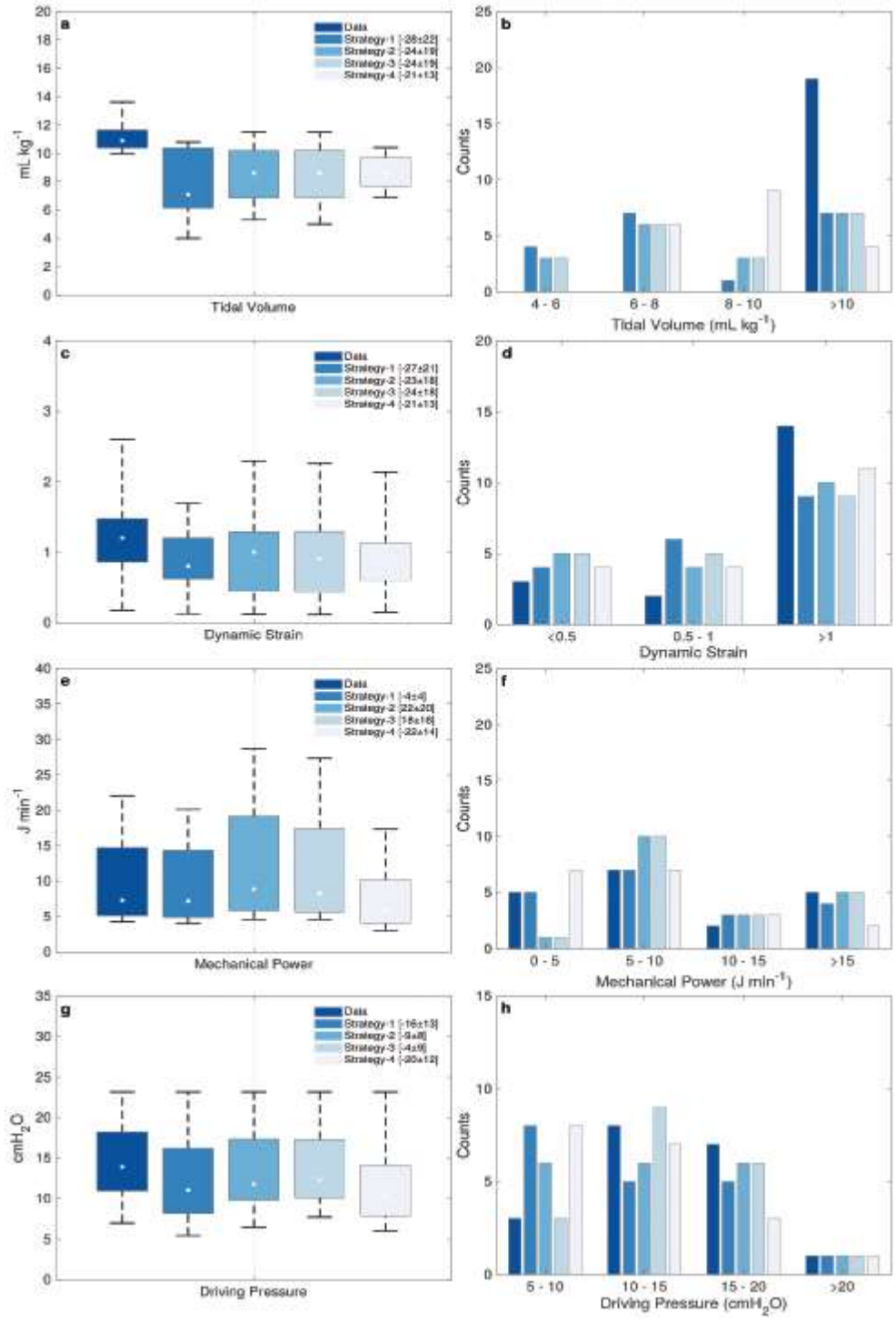

Figure S7: Test Cohort 2, box plots on the left show data as median, interquartile range and actual range while histograms on the right demonstrate the distribution of all patients' data before and after implementing different strategies. Numbers in the brackets are the percentage of average change across the cohort [mean±SD]. Panels illustrate the amount of tidal volume reduction (a)-(b), comparison of the alveolar dynamic strain (c)-(d), change in

mechanical power (e)-(f) and driving pressure (g)-(h). Strategy-1: Reducing V_T whilst maintaining the initial minute ventilation; Strategy-2: Reducing V_T whilst maintaining the initial alveolar minute ventilation; Strategy-3: Reducing V_T whilst maintaining both the initial alveolar minute ventilation and inspiratory flow; Strategy-4: Reducing ΔP by increasing PEEP and decreasing V_T.